TOPICAL REVIEW • OPEN ACCESS

Bioink properties before, during and after 3D bioprinting

Biofabrication

TOPICAL REVIEW

Bioink properties before, during and after 3D bioprinting

Katja Hölzl[1,2,7], Shengmao Lin[3,6,7], Liesbeth Tytgat[4,5], Sandra Van Vlierberghe[4,5], Linxia Gu[3] and Aleksandr Ovsianikov[1,2]

[1] Institute of Materials Science and Technology, Technical University Vienna, Austria
[2] Austrian Cluster for Tissue Regeneration, Austria
[3] Department of Mechanical & Materials Engineering, University of Nebraska-Lincoln, USA
[4] Polymer Chemistry and Biomaterials Group, Ghent University, Belgium
[5] Brussels Photonics Team, Vrije Universiteit Brussel, Belgium
[6] School of Civil Engineering and Architecture, Xiamen University of Technology, China
[7] Both authors contributed equally to this paper.

E-mail: Aleksandr.Ovsianikov@tuwien.ac.at

OPEN ACCESS

RECEIVED
24 March 2016

REVISED
6 June 2016

ACCEPTED FOR PUBLICATION
20 July 2016

PUBLISHED
23 September 2016

Keywords: tissue engineering, bioprinting, hydrogels, scaffold, numerical modeling, bioink, 3D printing

Abstract

Bioprinting is a process based on additive manufacturing from materials containing living cells. These materials, often referred to as bioink, are based on cytocompatible hydrogel precursor formulations, which gel in a manner compatible with different bioprinting approaches. The bioink properties before, during and after gelation are essential for its printability, comprising such features as achievable structural resolution, shape fidelity and cell survival. However, it is the final properties of the matured bioprinted tissue construct that are crucial for the end application. During tissue formation these properties are influenced by the amount of cells present in the construct, their proliferation, migration and interaction with the material. A calibrated computational framework is able to predict the tissue development and maturation and to optimize the bioprinting input parameters such as the starting material, the initial cell loading and the construct geometry. In this contribution relevant bioink properties are reviewed and discussed on the example of most popular bioprinting approaches. The effect of cells on hydrogel processing and vice versa is highlighted. Furthermore, numerical approaches were reviewed and implemented for depicting the cellular mechanics within the hydrogel as well as for prediction of mechanical properties to achieve the desired hydrogel construct considering cell density, distribution and material–cell interaction.

1. Introduction

Fabrication of scaffolds by employing additive manufacturing technologies (AMT) also referred to as three-dimensional (3D) printing, has been widely used in tissue engineering to restore, replace or regenerate defective tissues [1, 2]. Bioprinting can be considered an additive manufacturing technique during which cells and biomaterials, often referred to as 'bioink', are deposited simultaneously [3, 4]. Bioprinting allows to skip the cell seeding procedure, which often proved to be challenging for classical scaffold-based tissue engineering. Moreover, it provides a possibility to distribute different cell types at desired locations within the bioprinted construct and achieve high initial cell densities. A number of comprehensive reviews, book chapters and books, discussing the relevant technologies and materials have been published over the years [3, 5–21]. In order, to achieve the desired tissue construct, it is essential to understand the properties of bioprinted hydrogel matrix and identify its key parameters (cell density, geometry, stiffness, etc) influencing tissue development and maturation.

In this review, recent progress in bioprinting and relevant bioink properties with focus on the interaction between hydrogel materials and cells is summarized. The properties of the hydrogel, which are required for the printing process as well as to ensure cell survival are discussed along with the influence of cells on the hydrogel properties itself.

We also describe a numerical approach allowing the estimation of the mechanical properties of a cell-containing hydrogel. The effect of cell densities and

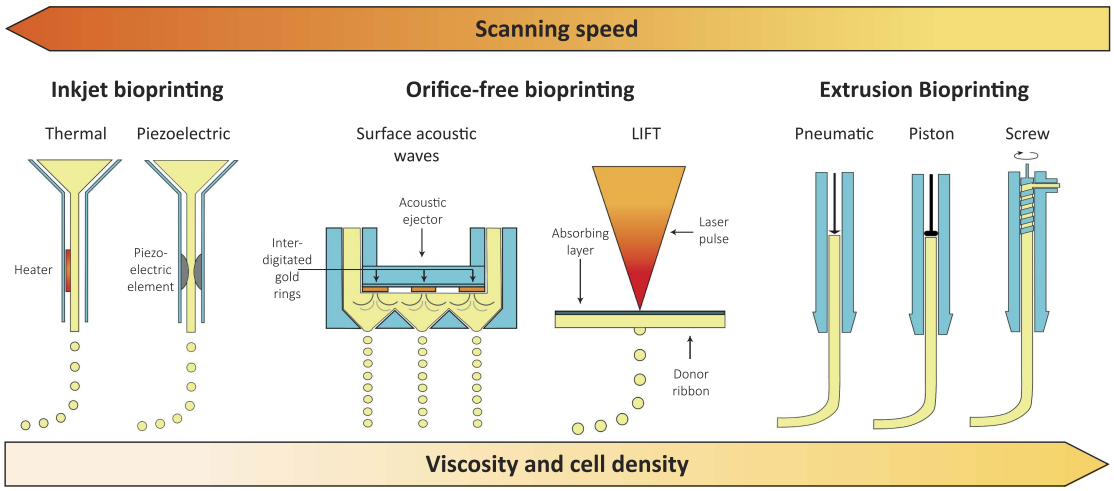

Figure 1. Overview of the most widespread bioprinting approaches and according parameters crucial for printability of the material.

distributions within the hydrogel was discussed, which might help to design the bioprinted constructs in a way to achieve the desired properties.

2. Overview of bioprinting methodologies and suitable bioink materials

The physico-chemical parameters of a hydrogel precursor including the rheological behavior, the swelling properties, the surface tension and the gelation kinetics are important factors for its printability. This especially applies for biofabrication techniques that rely on bioink dispensing. Therefore, different hydrogel properties are essential depending on the particular bioprinting technique to be applied. With regard to that, such processing methodologies can be subdivided into three groups including extrusion bioprinting (pneumatic and mechanical), orifice-free bioprinting (laser-induced forward transfer (LIFT) and printing by surface acoustic waves) and inkjet bioprinting (piezoelectric and thermal) (see figure 1).

2.1. Inkjet bioprinting

An inkjet bioprinter delivers small droplets of bioink (1–100 picoliters; 10–50 μm diameter) [16, 22] on predefined locations of a substrate. The two most commonly used methods for inkjet printing of cells are piezoelectric and thermal inkjet bioprinting [6, 23, 24]. The piezoelectric inkjet printer uses piezoelectric crystals to produce acoustic waves to force the liquid in small amounts through the nozzle [16, 25–28]. The thermal inkjet system produces pulses of pressure by vaporizing the bioink around the heating element expelling the droplets out from the printing head. Several studies have already indicated that cells are not affected by the local high temperature of the heating element up to 300 °C due to the short period of exposure (2 μs) during the printing process [29–32].

In inkjet bioprinting the surface tension is an important parameter that determines to what extent the processing technology will result in the formation of droplets or a jet. Surface tension is the result of the cohesive forces existing between the compounds present in the liquid. When the charges on the surface of the bioink are weaker than the surface tension, droplets are formed. Conversely, a jet is produced. The surface tension decreases with increasing cell concentration in the bioink, because more cells are adsorbed to the liquid-gas interface. Therefore, the total free energy is reduced, resulting in a smaller surface tension [33].

Gelation methods including physical [27, 34], chemical and photo-crosslinking [35] are used to ensure the stability of bioprinted constructs. Gelation of the bioink should occur *in situ* after the material exits the nozzle and simultaneously with the printing process (e.g. by photopolymerization) [32], because when it already takes place inside the printing head, blockages are created in the nozzle [23]. When hydrogel formation does not occur rapidly *in situ* the bioprinted construct might be compromised due to possible spreading of non crosslinked bioink solution. Furthermore, the shear stress characteristic to this process can negatively influence the cell viability [36]. As a result, the bioink must exhibit low viscosities (<10 mPa s) and cell densities (<10^6 cells ml^{-1}) (see figure 1 and table 1) [29, 37, 38]. These conditions result in limitations for the printing process. Despite the disadvantages, inkjet bioprinters are successfully applied with a micrometer resolution (10–50 μm) [23, 28, 39] for the deposition of cells and are compatible with various bioinks [23, 29, 40].

2.2. Orifice-free bioprinting

LIFT is also known as laser-assisted bioprinting and biological laser printing. In LIFT a pulsed laser beam is focused and scanned over a donor substrate that is

Table 1. Overview of crucial bioink parameters, which are characteristic for the discussed bioprinting approaches. Adapted from [40].

	Orifice-free bioprinting			
	LIFT [41, 67, 68]	Acoustic [19, 48, 69]	Inkjet bioprinting [23, 29, 30, 37, 38, 61]	Extrusion bioprinting [7, 36, 53, 54, 57, 62–66]
Viscosity bioink	1–300 mPa s	1–18 mPa s	<10 mPa s	30–6 × 10^7 mPa s
Cell density	Medium (10^8 cells ml^{-1})	Low (<16 × 10^6 cells ml^{-1})	Low <10^6 cells ml^{-1}	High, cell spheroids
Resolution	10–100 μm	3–200 μm	10–50 μm	200–1000 μm
Single cell control	Medium	High	Low	Medium
Fabrication speed	Medium (200–1600 mm s^{-1})	Fast 1–10 000 droplets s^{-1}	Fast (100 000 droplets s^{-1})	Slow (700 mm s^{-1}–10 μm s^{-1})
Cell viability	>95%	89.8%	>85%	80%–90%

coated with an absorbing layer (e.g. gold or titanium) and a layer of bioink [41]. The focal point of the laser causes local evaporation of the absorbing layer thereby creating a high-pressure bubble that propels small portions of bioink towards a collector platform. The bioink jet extends towards the collector before separating from the donor substrate, by this way creating a temporary connection between both substrates [42–45]. This bioprinting technique is nozzle-free and is therefore not affected by clogging problems. Another substantial advantage is that the shear stress caused by the material passing through a nozzle (inkjet) or a needle (extrusion) is avoided. The resolution of LIFT is in the range of 10–100 μm [41, 45]. It is influenced by various factors, such as the laser parameters, the air gap between the donor substrate and the collector platform, the thickness and viscosity of the bioink layer [44]. LIFT is suitable for bioinks with a viscosity ranging from 1 to 300 mPa s and medium cell densities of ~10^8 cells ml^{-1} (table 1) [40, 41, 46, 47]. Understandably, bioprinting of well-defined 3D structures from low viscosity bioinks might be quite challenging. For the fabrication of the predesigned 3D constructs at high spatial resolution the bioink must exhibit fast crosslinking. Among the suitable cross-linking mechanisms, ionic crosslinking of sodium alginate containing bioink is frequently used. Also the temperature dependent gelation of Matrigel or enzymatic driven polymerization of fibrinogen were demonstrated [41, 42, 46].

Another elegant orifice-free bioprinting technique is relying on surface acoustic waves [19, 48]. The latter are produced by an acoustic ejector, which uses a surface acoustic wave piezoelectric substrate (e.g. lithium niobate, quartz, etc) with interdigitated gold rings placed on top of the substrate. Due to the circular geometry of the waves, an acoustic focal plane is generated at the air-liquid interface in the microfluidic channel. As a result, the bioink droplets are ejected from the microfluidic channel. The diameter of the droplets is uniform and can be set between 3 and 200 μm by changing the wavelength of the acoustic ejector. The embedded cells are not exposed to nozzle geometry, heat or high pressure, which results in a high cell viability (>89.8%). Furthermore, bioinks with various surface tensions and viscosities can be ejected [19, 48].

2.3. Extrusion bioprinting

Perhaps the most widespread method for the fabrication of 3D cell-laden constructs is extrusion bioprinting [41, 49]. For extrusion bioprinting, the bioink is generally inserted in disposable plastic syringes and dispensed either pneumatically or mechanically (piston- or screw-driven) on the receiving substrate [15]. In contrast with a LIFT or an inkjet bioprinter, an extrusion bioprinter does not dispense small bioink droplets but rather larger hydrogel filaments (approximately 150–300 μm in diameter) [16, 50–54]. A piston-driven system may provide more direct control over the flow of the bioink, when compared to pneumatic-based systems, prone to delays associated with the compressed gas volume. Screw-based deposition provides more spatial control and is capable of dispensing bioinks exhibiting higher viscosities [12]. However, the larger pressure drops generated by this extrusion method can be harmful for the suspended cells due to possible disruption of the cell membranes which results in cell death [55]. Because of the possibility to adjust the air pressure, pneumatic deposition can be used for a broad range of bioink types and viscosities. Advantages of extrusion bioprinting include the ability to print viscous bioinks (30 –6 × 10^7 mPa s) with very high cell densities, and even cell spheroids, into 3D scaffolds (see figure 1 and table 1) [40, 56]. The drawbacks related to this approach are its inferior resolution (200–1000 μm), potential nozzle clogging and the decreased cell viability due to shear stress [12, 40, 57]. The crosslinking pathways for fixation include physical (shear thinning and thermally induced), chemical (e.g. Michael addition reactions, click chemistry, etc) and photo-induced crosslinking [16, 40].

Another common aspect is that bioink formulations having adequate mechanical properties for

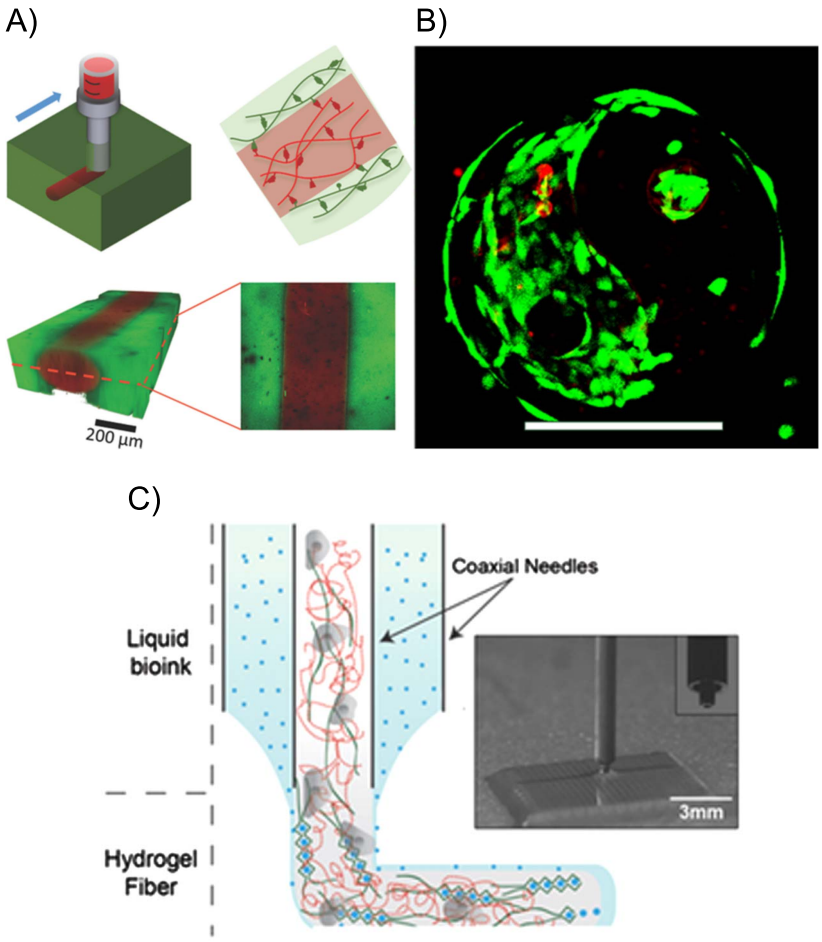

Figure 2. (A) Extrusion of a shear-thinning bioink into a self-healing support hydrogel allowing printing of high-resolution and multimaterial structures encapsulating cells. Reproduced from [59] with permission of John Wiley and Sons. (B) Bioprinting using coaxial needle system. The inner needle contains the bioink consisting of gelatin methacroyl (red dashed lines), alginate (green lines), photoinitiator and cells. The outer needle contains the $CaCl_2$ (blue dots), which induces gelation after mixing. Reproduced from [58] with permission of John Wiley and Sons.(C) Proliferation of cells in a construct printed using two-photon polymerization, scale bar 200 μm (right) [60].

fabrication of stable 3D constructs at good bioprinting accuracy often present suboptimal environment for cell migration and spreading [12]. A new bioprinting approach, which might overcome some of these drawbacks was reported recently by [58, 59]. In this gel-in-gel bioprinting method bioink is extruded into a volume of self-healing hydrogel acting as a support material. The support hydrogel deforms upon the injection of bioink and heals immediately after deposition enclosing the printed structure inside (see figure 2a). By using photocrosslinking as secondary stabilization step the mechanical properties of the printed construct can further be improved. Moreover, in combination with photocrosslinking, where either the bioink or the support hydrogel is photosensitive, freestanding 3D structures or structures with voids can be generated, by washing away the unstabilized hydrogel. This gel-in-gel printing method also opens up the possibility to print multiple materials and as the hydrogels are shear thinning also printing of cells results in a high viability (>90%).

2.4. Methods for hydrogel gelation

Hydrogel fixation (i.e. 'gelation') is an important aspect in preserving the shape of a bioprinted constructs thereby minimizing structure collapse [12]. The different gelation mechanisms can be subdivided into two categories being physical and chemical crosslinking. The network formation of a physical hydrogel is reversible and is the result of the occurrence of ionic interactions, high molecular chain entanglements, hydrogen bonds and/or hydrophobic interactions [70, 71]. Physically crosslinked hydrogels are usually associated with poor mechanical stability [55]. To overcome this limitation, chemical functionalities can be introduced to improve the mechanical strength of the hydrogel by creating covalent crosslinks, thereby resulting in an irreversibly crosslinked network [72, 73]. An irreversible network can be achieved by Michael-type addition reactions [74], click chemistry [75], enzymatic reactions [76] and photo-induced polymerization [77]. Li *et al* recently reported the development of a two-component bioink based on a supramolecular polypeptide–DNA hydrogel

Table 2. Overview of commercially available bioprinters.

Bioprinter and manufacturer	Fabrication technique	Specified resolution	Recommended materials
3Dn300TE, NScrypt	Extrusion-based	Line widths 20–100 μm	Not specified (viscosity range: 0.001–1000 Pa s)
3D-Bioplotter®, Envisiontec[a]	Extrusion-based	Minimum strand diameter 100 μm	Hydrogels, ceramic, metal pastes, thermoplasts
Bioscaffolder®, Gesim[a]	Extrusion-based	Not specified	Hydrogels, biopolymers (collagen, alginate) bone, cement paste, biocompatible silicones and metling polymers (CPL, PLA)
Biobot 1, Biobots[a]	Extrusion-based	Layer resolution 100 μm	Hydrogels, biopolymers (viscosity range: 100–10^4 Pa s, see table 3 for more details)
Inkredible+, Cellink[a]	Extrusion-based	Layer resolution 50–100 μm	Hydrogels (see table 3)
Biofactory®, RegenHU[a]	Extrusion-based Inkjet	Not specified	Bioink, Osteoink (see table 3 for more details)
Revolution, Ourobotics	Extrusion-based	Not specified	Collagen, gelatin, alginates, chitosan
Bio3D Explorers, Bio3D technologies[a]	Extrusion-based	Not specified	Not specified
CellJet Cell Printer, Digilab		Droplet size 20 nl–4μl	Water-based, hydrogels, alginate, polyethylene glycol
BioAssemblyBot, advanced solutions	Extrusion-based	Not specified	Not specified
Regenova, Cyfuse	Spheroid assembly	Related to spheroid diameter	Cells only (scaffold/biomaterial-free approach)
NovoGen MMX, Organovo[b]	Inkjet	20 μm	Cellular hydrogels
Dimatix Materials Printer, Fujifilm	Inkjet	20 μm	Water-based, solvent, acidic or basic fluids
Poietis[b]	LIFT	20 μm	Not specified

[a] Light curing system.

[b] Not for sale, but utilized for bioprinting human tissue.

[78]. A combination of both physical as well as chemical crosslinking can also be pursued [72, 79]. Physical crosslinking is generally used for biofabrication processes, since chemical crosslinking is often associated with stringent control over the crosslinking kinetics to avoid blocking of the nozzle [12]. Therefore, chemical crosslinking is frequently used as post-processing fixation and stabilization of the printed 3D constructs [55]. For example, Billiet *et al* already reported on the application of methacrylamide-modified gelatin which was exposed to post-processing photo-induced crosslinking to produce mechanically stable 3D-constructs [63]. Sometimes a two-step photopolymerization approach is used to create a viscous, yet printable bioink and then the printed construct is fully photopolymerized to obtain the final shape of crosslinked scaffold. Skardal *et al* used this two-step photopolymerization method to create 3D scaffolds based on a methacrylated ethanolamide derivative of gelatin and methacrylated hyaluronic acid for tissue engineering applications. First, the gelatin and hyaluronic acid derivatives were partially photocrosslinked to obtain a gel-like bioink. Then the desired constructs were printed and photocrosslinked completely to fix their shape [80].

Colosi *et al* has recently reported the use of low-viscosity bioink blend of alginate and gelatin methacroyl (GelMA) with a coaxial dispensing system [81]. GelMA at low concentrations (<5% w/v) exhibits favourable properties for cells, but is not printable. Combining it with alginate results in a bioink mechanically stabilized by physically cross-linked fibers. Coaxial needle system (figure 2c) allows to precisely tune the gelation kinetics of this bioink by adjusting concentrations of alginate and $CaCl_2$. After bioprinting the hydrogel construct is further reinforced by UV cross-linking of GelMA.

2.5. Commercialization of bioprinting

The recent progress along with the increased attention to the field of bioprinting lead to intensified commercialization of devices and materials. Table 2 provides an overview of some commercially available bioprinters with their specifications and typical printing materials. Currently there is no standard way for defining the resolution of the printing process. Hence, manufacturers provide different parameters to describe it. For future evaluation, standardized parameters have to be defined in order to reasonably compare different printing methods.

While most of these printing devices rely on a single biofabrication method, RegenHU offers the selection between different fabrication technologies or combinations thereof. Very often bioprinters are also equipped with an additional light source enabling photo-induced polymerization, also referred to as curing, of the specialized bioinks.

As bioprinting has been commercialized, companies also start to offer their own bioinks. Among these, materials based on various cross-linking

Table 3. Overview of commercially available bioinks.

Company	Bioink	Material	Features
Bioink Solutions, Inc.	Gel4Cell®	Gelatin-based	UV-crosslinkable Cell viability >90%
	Gel4Cell®-BMP	Conjugated with different growth factors	Osteoinductive
	Gel4Cell®-VEGF		Angiogenic
	Gel4Cell®-TGF		Chondrogenic
CELLINK	CELLINK	Nano-cellulose/alginate mixture	Shear thinning Fast crosslinking For soft tissue engineering
RegenHU	BioInk®	PEG/gelatin/hyaluronic acid-based	Good cell adhesion properties Biodegradable Mimics the natural ECM Possible combination with Osteoink™
	Osteoink™	Calcium phosphate paste	Osteoconductive Chemical composition similar to human bone For hard tissue engineering
Biobot	Bio127	Pluronic F127-based	Gels at room temperature Dissolves when cooled
	BioGel	Gelatin Methacrylate based	When combined with GelKey it Covalently crosslinks when exposed to light

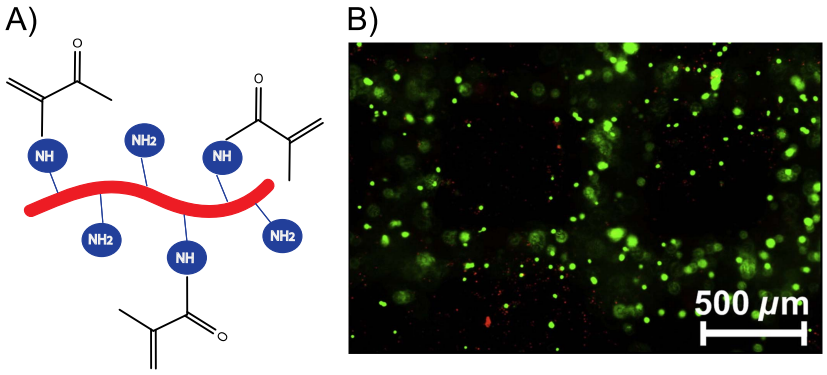

Figure 3. (A) Structure of gelatin modified with methacrylamide groups (Gel-MOD). (B) Hepatocarcinoma cell were encapsulated in Gel-MOD constructs and cured using Irgacure 2959. Cell survival was evaluated with live/dead assay [63].

mechanisms and specified for different applications can be found (table 3). For example Bioink Solutions, Inc. offers gelatin-based bioinks containing growth factors that are specific for the printing of different tissue types.

Rheological properties of these bioinks are mostly not indicated by the manufacturer. Therefore, they might only be suitable in combination with the companies own bioprinter and would have to be adapted for other printing techniques.

Generally, these bioinks are constituted from natural and/or synthetic polymers including collagen/gelatin, hyaluronic acid, PEG, etc. Collagen is the most abundant protein present in the extracellular matrix (ECM) of many tissues [82]. This protein forms a hydrogel at physiological conditions by triple helix formation. Collagen is a suitable material for cell encapsulation purposes because of the presence of cell-interactive RGD (Arginine-Glycine-Aspartic acid) sequences in their backbone, which stimulate cell adhesion. For example, Xu *et al* have mixed rat embryonic hippocampal neurons with neutralized collagen and placed the cell-laden solution subsequently in the incubator at 37 °C to induce hydrogel formation [83]. The degradation of the triple helix of collagen by acidic or basic hydrolysis results in the production of gelatin [71]. Gelatin is a thermoresponsive protein with a sol-gel temperature of around 30 °C depending on the gelatin concentration applied. By cooling a gelatin solution below 30 °C, hydrogel formation is induced (cfr. upper critical solution temperature behavior) [84]. This protein is often employed for tissue engineering and regenerative medicine because various functional groups corresponding with constituting amino acids can be easily modified with (meth)acrylate groups to prevent

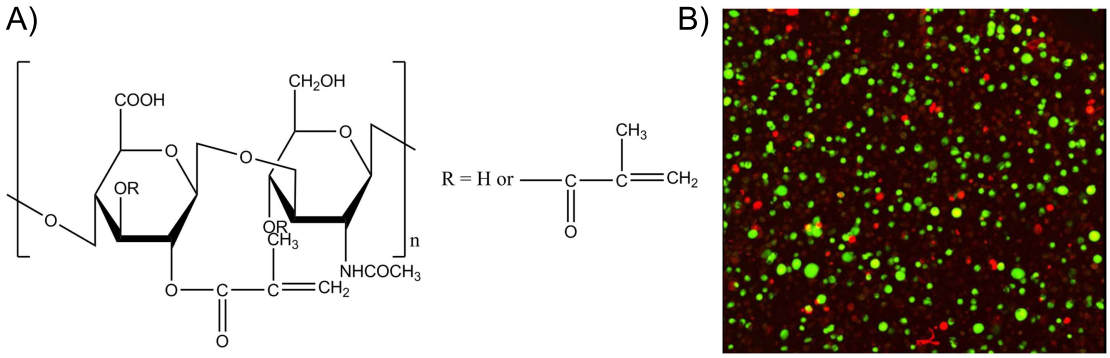

Figure 4. (A) Structure of methacrylated hyaluronic acid. (B) Live/dead staining results indicated that encapsulated cardiac valvular interstitial cells in methacrylated hyaluronic acid hydrogels remained viable after 1 week of cell culture [87].

liquefying of gelatin at physiological temperature [60, 63, 77]. In addition, gelatin is bio-interactive due to the presence of RGD sequences (figure 3).

Not only proteins are present in the ECM, but also glycosaminoglycans including hyaluronic acid, which is a biodegradable, biocompatible and non-immunogenic biopolymer. The modification of hydroxyl and carboxylic acid functional groups of hyaluronic acid enable the introduction of photocrosslinkable moieties which can be photopolymerized in the presence of cells [85, 86]. Masters *et al* for example investigated the effect of photocrosslinkable methacrylated hyaluronic acid hydrogels on the cell response of encapsulated cardiac valvular interstitial cells (figure 4). Results showed that after 1 week, the embedded cells were still viable indicating the potential of these materials for tissue engineering purposes [87].

Also synthetic polymers such as PEG-based hydrogel precursors have already been frequently used for cell encapsulation because their mechanical, swelling and diffusion properties can be easily controlled by varying the crosslinking degree. On the other hand, these hydrogels lack inherent binding sequences, like the common RGD motif, for cell attachment and are not degradable. To make them more suitable for cells, these hydrogels have to be modified with the necessary binding peptides and enzymatically degradable groups. For example, Bryant *et al* developed PEG diacrylate hydrogels and incorporated RGD sequences in the backbone to enhance the cell-interactive properties of the hydrogel [88].

2.6. Summary

Each bioprinting technique has its own set of 'ideal requirements' with respect to the bioink properties, in order to achieve designed 3D geometries with the desired resolution and a high viability of the embedded cells (see table 1). In addition, process peculiarities might necessitate more specific material characteristics. A plethora of rheological parameters (i.e. viscosity, shear thinning and thixotropy) can be distinguished, which inherently affect the bioprinting process [12]. Viscosity is determined by temperature, the polymer concentration and its molecular weight. A bioink exhibiting a high viscosity is associated with an increased shear stress during the printing process, which can cause cell damage [89]. A previous study has already shown that the viscosity of a cell-laden hydrogel influences shape fidelity after deposition. Low-viscosity bioink forms strands which spread out on the receiving platform, while higher viscosity bioinks leads to the formation of filaments on the collecting substrate [90]. The viscosity of shear thinning materials decreases with increasing shear rate. This property results in high printing fidelity, because the applied pressure in the nozzle causes a decrease in viscosity thereby facilitating the deposition of the bioink. As the shear stress is removed after exiting the orifice, the viscosity increases sharply [18, 64]. This effect also takes place for thixotropic biomaterials, for which the decrease in viscosity is reversible and time-dependent [91]. Therefore, these phenomena are extremely useful for nozzle-based applications.

For example, inkjet bioprinting exhibits limitations regarding the material viscosity, while extrusion-based techniques may require shear-thinning properties to reduce the shear stress on the embedded cells to increase the cell viability [92]. The low viscosity bioinks for inkjet bioprinting require fast crosslinking mechanisms to facilitate the layering of the 3D-printed constructs. Conversely, crosslinking in extrusion bioprinting can be executed after fabrication, because the high viscosity bioinks maintain their 3D shape after deposition [12, 40]. However, the resolution of extrusion bioprinting is directly related to the diameter of the needle, which might result in some restrictions on material viscosity and affect the shear-stress induced during the dispensing process. Another interesting option is gel-in-gel bioprinting, allowing to extrude soft cell-friendly bioinks into the support gel. It remains to be seen how the supporting gel volume displaced by deposited bioink would affect the bioprinted construct in case when a large bioink quantity is used. By using a combination where one of the two

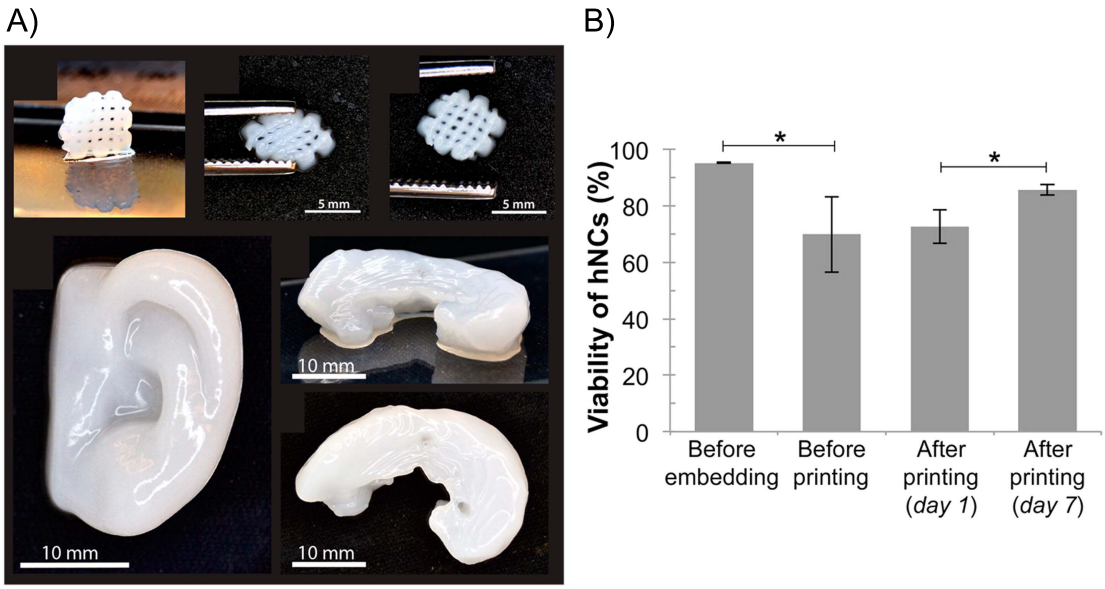

Figure 5. (A) 3D printed constructs of the nanofibrillated cellulose/alginate bioink that show stability in size and shape. (B) Viability of hNSCs before and after the printing process. Reprinted with permission from [100]. © 2015 Reprinted with permission from American Chemical Society.

hydrogels is photopolymerizable, gel-in-gel printing allows to create constructs with localized photosensitivity. As a results a photopolymerizable part of the construct can be crosslinked, while the rest of the material is washed away to reveal the desired structure. A similar outcome is achieved by lithography-based 3D printing technologies. In this case it is not necessary to combine different properties, instead the same hydrogel is crosslinked selectively by controlling the material-light interaction volume [17]. Somewhat higher spatial resolution and true 3D structuring, without the necessity to deposit material layer-by-layer, is possible with multi-photon processing [93]. For example gelatin-based bioinks, already in their physical gel state, can be locally cross-linked by two-photon polymerization (figure 2c) [60].

In the case of LIFT and inkjet bioprinting techniques bioinks also encounter localized heating, which can further affect the viability of cells. Therefore, bioinks with a low thermal conductivity may be applied, to facilitate cell viability and superior cell function after the printing process [94].

3. Hydrogel properties before and after bioprinting

The characteristics of the bioink should meet the mechanical requirements for the bioprinting process and at the same time ensure cell survival within the produced construct [95, 96]. Therefore, cytocompatibility of a bioink is another critical aspect concomitant with bioprinting. Hydrogels are commonly used for tissue engineering and biofabrication because of their high water content and low toxicity rendering them excellent mimics of the ECM [97, 98]. Several studies have already demonstrated that 3D hydrogels produced by a bioprinting technology, provide an excellent matrix for encapsulated cells [63, 99–101]. Malda *et al* gives a good overview of the cytocompatibility of different hydrogels when fabricated with different methods [12]. For example, 3D printed cell-encapsulating methacrylamide-modified gelatin hydrogels with a substitution degree of 62% resulted in a cell survival of >97% and maintained cell expression of the liver-specific functions.

Thus, the cell viability was not impaired due to the printing process (e.g. needle type, temperature, etc) and the exposure to increased fluid shear stresses [63]. In addition, Hsieh *et al* have shown that neural stem cells embedded in 20%–30% polyurethane hydrogels exhibit excellent proliferation and differentiation due to the low matrix stiffness. The developed hydrogel was anticipated to mimic the microenvironment of the brain, resulting in an excellent niche for neural stem cells [99]. Markstedt *et al* studied the use of a bioink that combined the outstanding shear thinning properties of nanofibrillated cellulose with the fast crosslinking ability of alginate. The printed constructs were stable in their shape and size and the embedded human chondrocytes exhibited a cell viability of 86% 7 d after printing (see figure 6). They stated that the bioink was suitable for 3D printing in the presence of living cells for inducing the growth of cartilage tissue [100]. Furthermore, Das *et al* assessed the differentiation potential of human nasal inferior turbinate tissue-derived mesenchymal progenitor cells embedded in silk fibroin-gelatin. In the latter, bioink gelation was induced via enzymatic crosslinking by mushroom tyrosinase and physical crosslinking via sonication (see figure 5). The results showed that the constructs

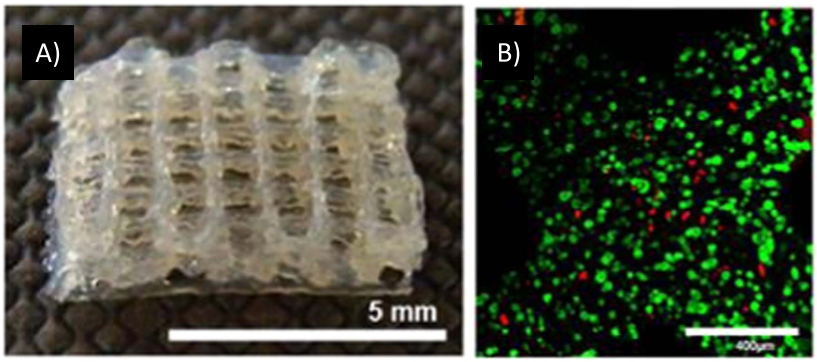

Figure 6. (A) 3D bioprinted silk-fibroin construct and (B) live/dead staining of hTMSCs encapsulated in the hydrogel [101].

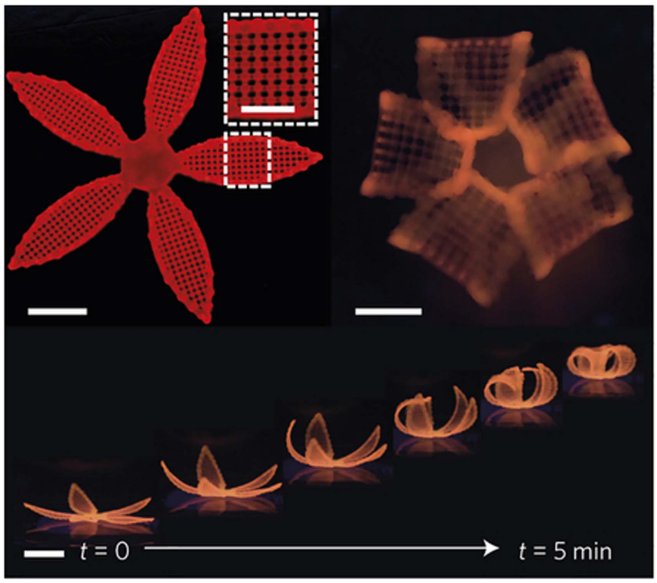

Figure 7. Constructs printed with inherent anisotropy due to spatial control of cellulose fibrils, leading to controlled shape change upon immersion in water. © 2016 Reprinted with permission from *Nature* [107].

supported multilineage differentiation of the encapsulated stem cells and specific tissue formation [101].

In clinical applications direct injection of cells within a carrier solution often leads to a low cell viability due to mechanical disruption of cell membrane. Mechanical properties of a hydrogel carrier can be designed in a way that protects cells during injection. Aguado *et al* shows the protective effect of crosslinked alginate hydrogel with different storage modulus on encapsulated cells. The cell viability after injection was significantly higher in all the crosslinked hydrogel carriers with G' ranging from 0.33 to 58.1 Pa compared to control samples where a cell suspension in PBS was injected. Cells encapsulated in the hydrogel with a storage modulus of 29.6 Pa showed the highest viability demonstrating the impact of cell carrier mechanics on the cell viability [89]. Also Yan *et al* investigated the flow profile of a ß-hairpin peptide-based hydrogel and could show their big potential as cell carriers for injection due to their shear-thinning and self-healing properties [102]. Moreover, Burdick group designed a Dock-and-Lock mechanism to obtain a self-assembling, self-healing and shear-thinning hydrogel for needle injection. Encapsulated mesenchymal stem cells showed a viability of >90% and remained homogenously distributed in the gel after needle injection [103].

Another important physico-chemical parameter for the fidelity of bioprinted constructs is the swelling behavior of hydrogels, which is mainly determined by the crosslinking extent and the charge densities [104]. This characteristic influences the final shape and the size of the printed 3D construct [90].

Moreover, the use of high levels of crosslinking result in lower swelling ratios thereby reducing the diffusion of oxygen and nutrients required for the cells to survive as a result of the reduced pore sizes [105]. Diffusion of waste products away from the cells encapsulated in the hydrogel is also managed in this context [97]. In addition, highly cross-linked hydrogels,

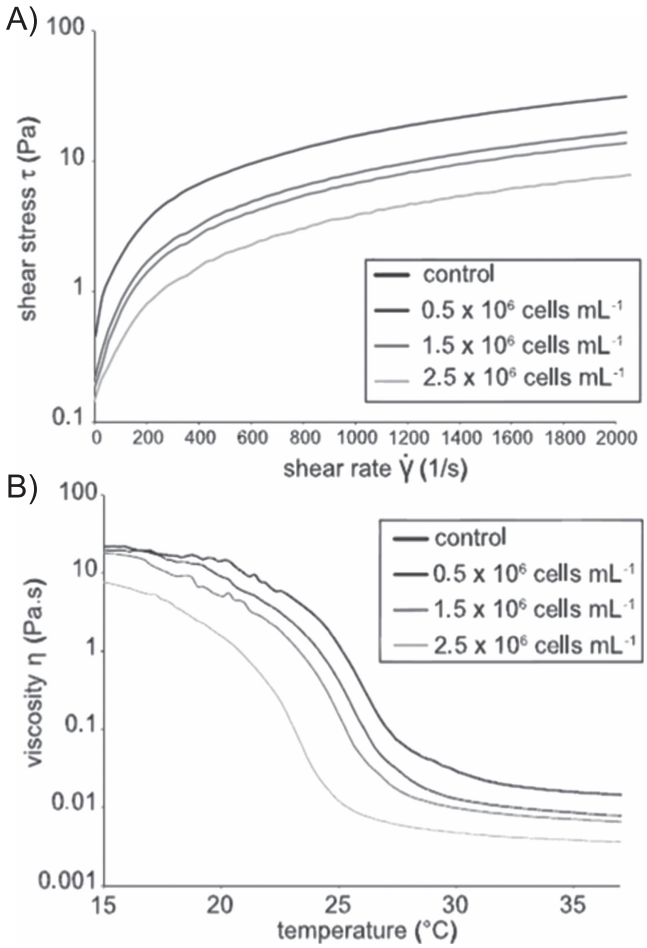

Figure 8. Influence of cell density on rheological properties of the hydrogel. (A) Correlation of cell density and shear stress as a function of shear rate and (B) viscosity as a function of temperature [63].

providing good shape fidelity after bioprinting, might not always be optimal from biological perspective due to impairment of cell migration and proliferation [12]. The requirements towards the properties of a hydrogel with regard to bioprinting process and cell culture are often opposing. A possible solution to this issue is combining hydrogels optimized for cell culture with materials providing mechanical stability and facilitating shape fidelity [106].

In a method referred to as 4D-Printing, Lewis *et al* demonstrated that by controlling swelling anisotropies within a hydrogel construct it can deform in controllable manner. Swelling anisotropy was introduced during printing by spatial control over the orientation of the cellulose fibrils inside the hydrogel. Upon immersion in water the structure swells and acquires its final shape over time (see figure 7) [107]. In general every bioprinting process has a 4D printing character since, it is likely that the geometry and properties will change in long term, unless completely isotropic constructs are built. For example the change in the geometry induced by swelling of zonal hydrogel constructs with different mechanical properties in separate layers has to be taken into account if swelling would occur after bioprinting [108].

4. Effect of cell content on material processing

It is expected that high initial density of cells in the bioprinted construct will lead to faster tissue formation. However, the presence of cells significantly affects the printability of bioinks. Indeed, Billiet *et al* have compared the processing potential of methacrylamide-modified gelatin (Gel-MOD) with and without hepatocarcinoma cells. It was demonstrated that the incorporation of the cells altered the rheological properties. As such, this parameter will affect the printing process since the viscosity is altered. For temperatures above the gelation point, the viscosity was reduced by a factor of 2, up to a cell density of 1.5×10^6 cells ml^{-1}. Increasing the cell density further to 2.5×10^6 cells ml^{-1} resulted in a further viscosity decrease up to a factor of 4 (see figure 8) [63]. Furthermore, Skardal *et al* have assessed the effect of the presence of human intestinal epithelial cells on hyaluronan-based hydrogels which were crosslinked using tetrahedral polyethylene glycol tetracrylate. Their report states that cell densities above a certain threshold, interfere with hydrogel formation. Bioink with cell densities up to 25×10^6 cells ml^{-1} formed

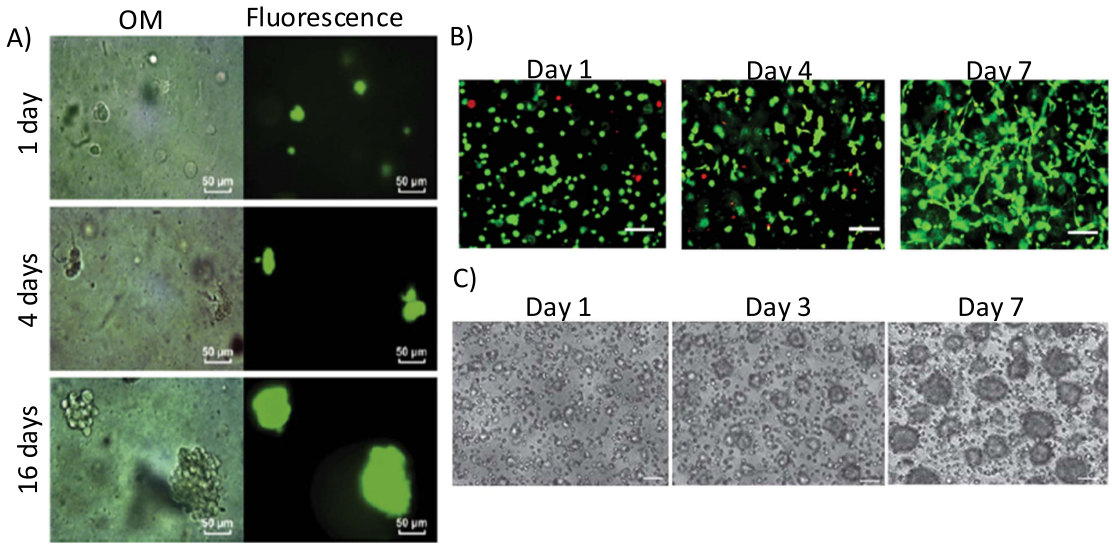

Figure 9. Cell proliferation in different hydrogels. (A) Optical and fluorescence microscopy images of MC3T3-E1 cells encapsulated in alginate beads treated with live/dead stain. © 2016 Reproduced with permission of The Royal Society of Chemistry [116]. (B) Fluorescent images of fibroblasts encapsulated in gelatin methacrylate (GelMA). © 2016 Reprinted with permission of John Wiley and Sons [117]. (C) Phase contrast images of 3D cell aggregate formation of 3T3-fibroblasts-laden 15% PulMA hydrogels [118].

hydrogels within 20 min. At higher cell densities the hydrogels did not form under the applied conditions [109].

The equilibrium and dynamic modulus at 1 Hz of agarose hydrogels with chondrocyte density at 0, 10, 40 million cells ml^{-1} were presented in the study by Buckley *et al* [110]. By maintaining the effective concentration of agarose as constant, both the equilibrium modulus and dynamics modulus at 40 million cells ml^{-1} were lower than acellular constructs. This result could be explained by the Young's modulus of a chondrocyte, which has been reported as approximately 0.6 kPa [111], an order of magnitude lower than that of agarose. In this case, a larger cell-seeding density would reduce the modulus of cell seeded agarose.

5. Predicting properties of hydrogels containing living cells

There was a certain amount of effort dedicated to predicting properties of the 3D printed scaffolds [112–115]. The mechanical properties of scaffolds were mainly considered with regard to construct compliance, but also in terms of cell-material interaction.

In case of bioinks one has to consider the presence of living cells not only with regard to bioprinting, but also in terms of possible long-term changes of bioprinted construct properties due to cell proliferation, migration and interaction with hydrogel material (cell traction, enzymatic degradation matrix remodeling). As shown in figures 9(A)–(C) there are different ways for cells to proliferate inside the hydrogel construct. For example MC3T3-E1 cells were found to grow in clusters when encapsulated in alginate hydrogel. In contrast, fibroblasts encapsulated in methacrylated gelatin were able to spread through the hydrogel over time, whereas they were found to grow in aggregates in pullulan methacrylate [116–118]. This behavior is not only attributed to the cell type, but also to the properties of the hydrogels, such as porosity, stiffness and most important the presence of ligands facilitating cell attachment.

The relationship between the density of encapsulated cells and mechanical properties of the resulting hydrogels was investigated by Mauck *et al* [119]. In their work, chondrocyte-seeded agarose hydrogels were cultured in free-swelling and dynamic loading conditions over a 2 month culture period. Constructs containing 10 million cells ml^{-1} were initially twice stiffer than the ones seeded with 60 million cells ml^{-1}. After culturing 56 d, the constructs seeded with more cells showed similar Young's modulus with the lower cell density one under the condition of free-swelling (85.1 $\pm$ 15 kPa versus 78 $\pm$ 1.5 kPa). This indicated that higher cell-seeding density accelerates the hydrogel remodeling. This observation was confirmed by Chang *et al* [120], who demonstrated that a higher cell density led to a larger equilibrium modulus of tissue implants after 30 weeks of culture. In addition, the dynamic loading condition resulted in a much larger Young' modulus for the hydrogel containing higher cell density (186.2 $\pm$ 11.3 kPa versus 91.5 $\pm$ 11.6 kPa). The loading condition induced dynamic modulus followed the same trend. The interesting observations were that both proteoglycan and collagen density remained the same regardless of free-swelling or dynamics loading. This was speculated that the loading condition promoted the production of linker

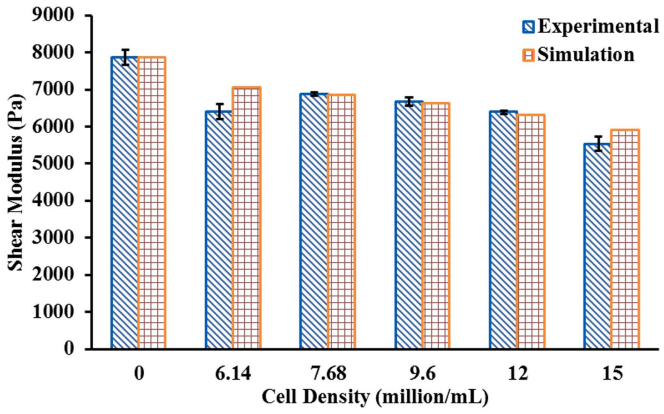

Figure 10. Predicted as well as experimentally measured shear modulus (Pa) for gels containing various cell densities (million ml^{-1}).

molecules and/or the aggregation of macromolecular proteoglycan. This work indicated that various cell densities encapsulated in the 3D hydrogel could promote material remodeling depending on external loading conditions. The experimental data reported in literature is generally obtained following different protocols, which makes it difficult to guide hydrogel design and optimization. Numerical models have the potential to predict mechanical properties of a construct with different cell density under various protocols. It is especially appealing considering the multitude of bioinks used by different groups and the diversity of their properties. Guilak *et al* [121] developed a finite element model of chondrocytes within an explant of cartilage to understand the interactions between cell and matrix, which differ by nearly three-order of magnitude in terms of their Young's modulus. This material mismatch resulted in stress concentrations at the cell-matrix interface. The consideration of a thin layer of pericellular matrix could alter the local mechanical environment of chondrocytes, suggesting a functional biomechanical role for the pericellular matrix. Another numerical model developed by Chang *et al* [122] provides a good base to evaluate mechanical properties of the hydrogel containing living cells. A strain energy density based damage criterion was proposed to correlate cellular viability with external loadings. However, the effect of cell density on the mechanical properties of the resulting construct as well as the cellular viability remains unclear.

Owing to the influence of loading the hydrogel construct with cells, we have studied this effect on the example of methacrylamide-modified gelatin (Gel-MOD) photopolymerized with the photoinitator LiTPO-L. The Gel-MOD loaded with different densities of MC3T3-E1 cells, ranging from 15 to 6.14×10^6 cells ml^{-1}, was characterized compared to acellular hydrogels using a photorheometer. The details of experimental procedure are similar to the ones reported previously by our group [123]. In short, the cells were directly resuspended in a 10% (w/w) Gel-MOD solution. Measurement of the storage modulus G' and the loss modulus G" were taken with a photorheometer (Anton Paar MCR 302 WESP) during a dynamic time sweep at a frequency of 10 Hz and strain of 10% during 10 min of photopolymerization with a 320–500 nm light source.

Our results presented here (previously unpublished) show that the stiffness of hydrogel drops by 13% when the cell density is increased from 12 to 15 million cells ml^{-1} (figure 10). Calibrated by the aforementioned experimental data, numerical models were developed to predict mechanical properties of hydrogels containing different cell densities and the corresponding cellular mechanics.

A representative volume element (RVE) of the hydrogel with side length of 150 μm was used to represent hydrogels containing different cell densities (figure 11). The encapsulated cells were modeled as solid sphere with 30 μm in diameter and 1.5 kPa in Young's modulus, which was adopted from the previous experimental observation on MC3T3-E1 cells [124]. Based on the aforementioned experimental measurements, the shear storage modulus and loss modulus of the acellular hydrogel was 7870 Pa and 11 Pa, respectively. In the model, the material behaviors of hydrogel were then defined by the magnitude of shear modulus and the Poisson's ratio of 0.49. A 10% shear loading was applied on the RVE to mimic the testing condition. Nonlinear finite element models were solved using ABAQUS 6.12 (Simulia, Providence, RI, USA). Different cell densities varying from 6.14 to 15 million ml^{-1}, corresponding to the volume fraction of 8.68% to 21.2%, were considered in the RVE. The estimated shear modulus of the RVE was found to be in good agreement with experimental measurements (figure 10). Both experiment and simulation demonstrated that higher cell density led to reduced modulus of the hydrogel. These findings are also consistent with experimental observations reported by other groups [63, 110, 119].

As cells are not always distributed homogeneously, but might be present in clusters inside the hydrogel,

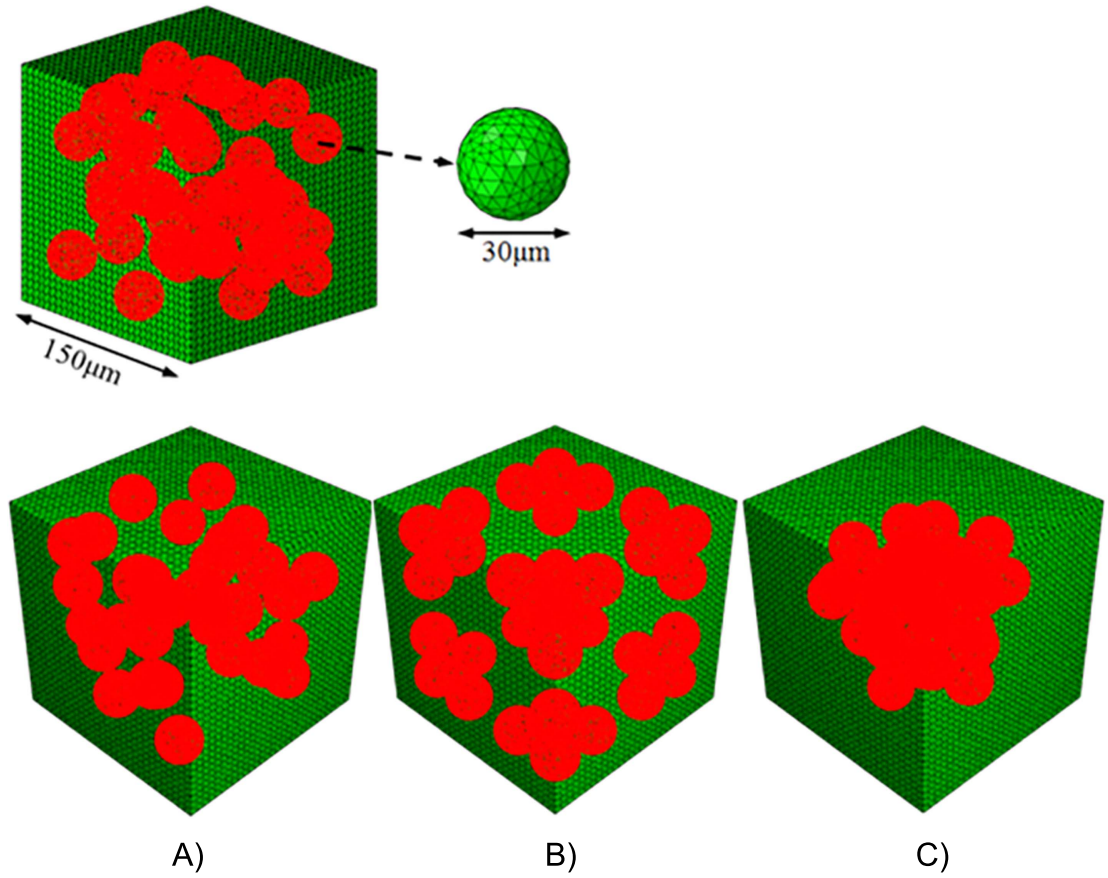

Figure 11. Representative volume element (RVE) used for numerical model of hydrogel containing randomly distributed cells at density of 12 million ml^{-1} (top). Numerical models of hydrogel containing living cells distributed (A) randomly, (B) in eight corner clusters and (C) in one central cluster at a density of 9.6 million ml^{-1}.

Table 4. Mechanical performance of hydrogel with different cell distribution.

	Random distributed	Edge clusters	Central cluster
Shear modulus (Pa)	6628	6141 (−7.3%)	6221 (−6.1%)

the effect of different cell distributions on the hydrogel properties was also investigated. This was illustrated by comparison of three different cellular distributions (random distributed, corner clusters and central cluster) at the same cell density of 9.6 million ml^{-1} as shown in figure 11. The obtained shear modulus from finite element models was summarized in table 4. It is clear that the samples with cell clusters are softer compared to the ones without randomly distributed cells.

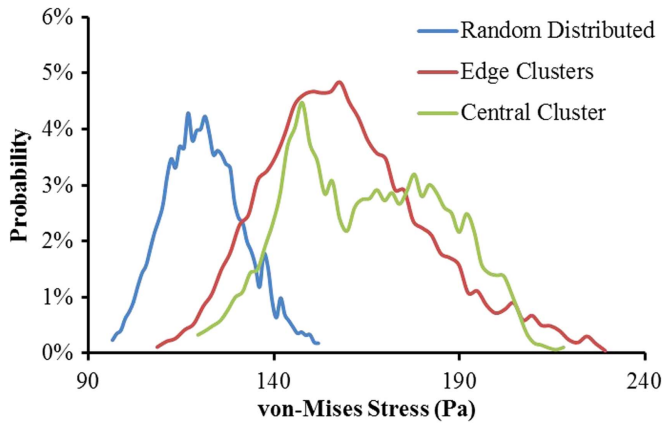

Figure 12. Probability distribution of von-Mises stresses on cells.

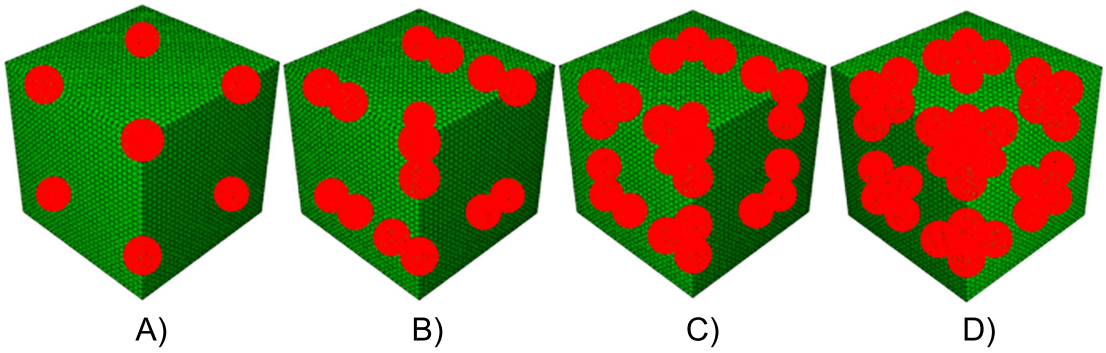

Figure 13. Numerical modeling of cell clusters forming within hydrogels as a result of cell proliferation. From left to right the representative volume elements (RVEs) containing 8; 16, 24, and 32 cells respectively.

Table 5. Mechanical performance of hydrogel with cell proliferation.

	Base	Double	Triple	Quadruple
Shear modulus (Pa)	7425	7010 (−5.6%)	6610 (−11.0%)	6141 (−17.3%)

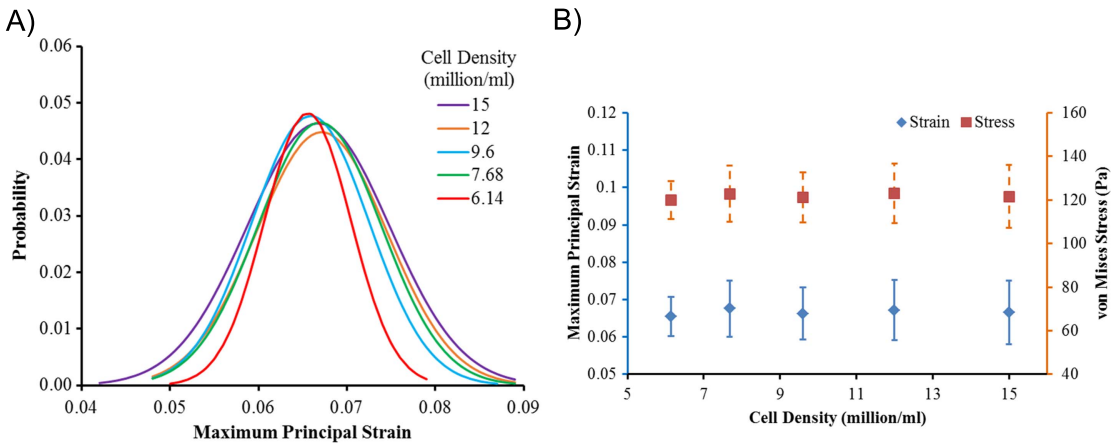

Figure 14. Loading sensed by cells encapsulated in a hydrogel at various densities (million ml^{-1}). (A) Probability distribution of maximum principal strain on cells; (B) mean maximum principal strain and von Mises stress (Pa) on cells.

The shear modulus for edge clusters and central cluster are 7.3% and 6.1% less than the Gel-MOD samples with random distributed cells. The minimal difference between two cluster distributions could be explained by the average distance between cells, which are close enough resulting in similar cell–cell interactions. The mechanical stresses sensed by cells embedded in Gel-MOD were depicted as probability curves in figure 12. It is obvious that cell clusters shifted probability distribution curve to a higher stress region. This implied that cells in cluster state are more prone to damage and therefore also more susceptive to mechanical stimulation. This behavior might be beneficial considering the matrix design for cartilage tissue engineering [125].

Moreover, multiple edge clusters shared a little larger loadings than the one central cluster, as indicated by the shapes of probability curves. However, in general the cluster distribution has minimal impact on the accumulated cellular loadings.

The formation of cell clusters inside the hydrogel might also result from proliferation of encapsulated cells (see figure 9). In order to estimate to what extent clusters might influence the temporal properties of the construct, the effect of cell proliferation was investigated by simulating four different situations related to cell division: initial distribution of single cells (8 cells per RVE), cell doubling (16 cells) etc (figure 13). Although this model might be not taking into account all the aspects of the cell–material interaction, it estimated that within the simulated range the shear modulus decreased from 7.425 to 6.141 kPa as a results of cell proliferation (see table 5). Since cell proliferation is imperative to most bioprinting methods it is important to be able to estimate the final mechanical properties of the construct based on the knowledge of initial material, cell density and proliferation rate. In addition, the appropriate numerical models should be capable of predicting the effect of material degradation, matrix remodeling etc [126].

The loadings sensed by cells are relevant to their behavior, including cellular viability, differentiation, and damage etc. We have delineated the maximum principal strain sensed by cells encapsulated in hydrogel as probability curves (figure 14a). It is clear that the cellular strain tends to be more inhomogeneous as the cell density increased. Higher strain regions were observed at the interface between the cell and hydrogel. This could be explained by the material mismatch between cell and hydrogel and the cell–cell interactions. Stress concentration was observed at the interface between cell and hydrogel, where there existed the material mismatch. Previous reports speculated, that this inhomogeneity is correlated with cellular damages as cells are more prone to be damaged at higher strain [122]. It is interesting to note though that mean stress and strain sensed by cells as a whole has no significant difference among various cell densities (figure 14b).

Another potentially important aspect of cell–material interaction, which might have an effect on the hydrogel construct, is cell contraction. Our modeling results assuming the 5% cell contraction (implemented as eigenstrain, which was estimated from the traction force microscopy data) showed only minimal effect on the mechanical properties of the hydrogel. Specifically, for the case of hydrogel containing 9.6 million cells, the cell contraction altered the shear modulus of the hydrogel from 6.628 to 6.631 kPa.

6. Future perspectives

The dawn of bioprinting enabled the generation and transplantation of several tissues, including multilayered skin, bone, vascular grafts, tracheal splints, heart tissue and cartilaginous structures [40]. Bioprinting has come a long way with the portfolio of bioinks designed for different technologies and applications expanding rapidly. Hydrogel properties relevant to the process of bioprinting have been systematically investigated and adapted to match different technologies. The development of the bioprinted construct into a tissue is gathered by a multitude of factors such as cell proliferation, material degradation, matrix remodeling etc. Although modern computational approaches should be capable of predicting these processes and benefiting the field of bioprinting, their development is currently lacking attention. Availability of according modeling tools would be highly advantageous, especially taking into account the diversity of bioink properties, expenditures associated with experimental optimization of bioprinted tissue constructs and the possibility to apply these tools to different geometries, e.g. patient-specific cases, in the future. This work reviewed the recent efforts aiming at predicting the properties of cell containing materials and constructs. Furthermore, we present an own model allowing to estimate the mechanical properties of hydrogels containing different cell densities and distributions. This model provides a fundamental framework for designing bioprinted constructs considering the impact of cell density to achieve desired mechanical properties. The model could be extended to incorporate complex 3D construct architectures, which has demonstrated great influence on their mechanical environments [127]. The predicted mechanical response of cells in various printed hydrogel architectures, integrated with experimental data, could be used to determine the cellular loadings, its damage threshold, as well as the longitudinal behaviors. In addition, the bioprinting process-induced mechanical disturbances has also been found to affect the cell viability [36]. Numerical modeling could be also used to mimic the mechanics during the fabrication process. Optimized parameters such as printing speed or nozzle diameter might be obtained for certain mechanical properties of hydrogel containing cells. In perspective, such computational tools can be directly integrated with modeling of tissue and organ development [128].

Disclosure of interests

We declare no potential conflicts of interest relevant to this article.

Acknowledgments

The authors acknowledge the financial support of the European Research Council (Starting Grant-307701, AO) and the National Science Foundation Faculty Early Career Development (award CBET-1254095: LG). We would like to thank The Research Foundation Flanders (FWO, Belgium) for providing a PhD fellowship to Liesbeth Tytgat. This work was also supported in part by FWO (G008413N, G044516N, G005616N, G0F0516N, FWOKN273), BELSPO IAP Photonics@be, the Methusalem and Hercules foundations, Flanders Make, the OZR of the Vrije Universiteit Brussel (VUB) and Ghent University (UGent). We would like to thank Prof. Jürgen Groll (Universitätsklinikum Würzburg) and Prof. Jürgen Stampfl (Technische Universität Wien) for their valuable comments, and Wolfgang Steiger (Technische Universität Wien) for his help with preparation of Figure 1.

References

[1] Chan B P and Leong K W 2008 Scaffolding in tissue engineering: general approaches and tissue-specific considerations *Eur. Spine J.* **17** 467–79
[2] Langer R and Tirrell D A 2004 Designing materials for biology and medicine *Nature* **428** 487–92
[3] Mironov V, Reis N and Derby B 2006 Review: bioprinting: a beginning *Tissue Eng.* **12** 631–4

[4] Groll J *et al* 2016 Biofabrication: reappraising the definition of an evolving field *Biofabrication* **8** 13001
[5] Atala A and Yoo J J 2015 *Essentials of 3D Biofabrication and Translation* (London: Elsevier)
[6] Campbell P G and Weiss L E 2007 Tissue engineering with the aid of inkjet printers *Expert Opin. Biol. Ther.* **7** 1123–7
[7] Chang C C, Boland E D, Williams S K and Hoying J B 2011 Direct-write bioprinting three-dimensional biohybrid systems for future regenerative therapies *J. Biomed. Mater. Res.* B **98B** 160–70
[8] Cho D-W, Lee J-S, Jang J, Jung J W, Park J H and Pati F 2015 *Organ Printing* (Bristol: IOP)
[9] Chua C K and Yeong W Y 2015 *Bioprinting: Principles and Applications* (NJ: World Scientific)
[10] Husár B, Hatzenbichler M, Mironov V, Liska R, Stampfl J and Ovsianikov A 2014 Photopolymerization-based additive manufacturing for the development of 3D porous scaffolds *Biomaterials for Bone Regeneration* (Amsterdam: Elsevier) pp 149–201
[11] Jakab K, Norotte C, Marga F, Murphy K, Vunjak-Novakovic G and Forgacs G 2010 Tissue engineering by self-assembly and bio-printing of living cells *Biofabrication* **2** 22001
[12] Malda J, Visser J, Melchels F P, Jüngst T, Hennink W E, Dhert W J A, Groll J and Hutmacher D W 2013 25th anniversary article: engineering hydrogels for biofabrication *Adv. Mater.* **25** 5011–28
[13] Mironov V, Visconti R P, Kasyanov V, Forgacs G, Drake C J and Markwald R R 2009 Organ printing: tissue spheroids as building blocks *Biomaterials* **30** 2164–74
[14] Narayan R 2014 *Rapid prototyping of biomaterials: principles and applications* (Cambridge: Woodhead)
[15] Ozbolat I T and Hospodiuk M 2016 Current advances and future perspectives in extrusion-based bioprinting *Biomaterials* **76** 321–43
[16] Pereira R F and Bártolo P J 2015 3D bioprinting of photocrosslinkable hydrogel constructs *J. Appl. Polym. Sci.* **132** n/a-n/a
[17] Qin X-H, Ovsianikov A, Stampfl J and Liska R 2014 Additive manufacturing of photosensitive hydrogels for tissue engineering applications *BioNanoMaterials* **15** 49–70
[18] Skardal A and Atala A 2015 Biomaterials for integration with 3D bioprinting *Ann. Biomed. Eng.* **43** 730–46
[19] Tasoglu S and Demirci U 2013 Bioprinting for stem cell research *Trends Biotechnol.* **31** 10–9
[20] Forgács G and Sun W 2013 *Biofabrication: Micro- and Nano-Fabrication, Printing, Patterning, and Assemblies* (Amsterdam; Boston: Elsevier/WA, William Andrew is an imprint of Elsevier)
[21] Jüngst T, Smolan W, Schacht K, Scheibel T and Groll J 2016 Strategies and molecular design criteria for 3D printable hydrogels *Chem. Rev.* **116** 1496–539
[22] Nakamura M, Kobayashi A, Takagi F, Watanabe A, Hiruma Y, Ohuchi K, Iwasaki Y, Horie M, Morita I and Takatani S 2005 Biocompatible inkjet printing technique for designed seeding of individual living cells *Tissue Eng.* **11** 1658–66
[23] Saunders R E and Derby B 2014 Inkjet printing biomaterials for tissue engineering: bioprinting *Int. Mater. Rev.* **59** 430–48
[24] Calvert P and Boland T 2012 *Biopolymers and Cells Inkjet Technology for Digital Fabrication* ed I M Hutchings and G D Martin (New York: Wiley) pp 275–305
[25] Lorber B, Hsiao W-K, Hutchings I M and Martin K R 2014 Adult rat retinal ganglion cells and glia can be printed by piezoelectric inkjet printing *Biofabrication* **6** 15001
[26] Saunders R E, Gough J E and Derby B 2008 Delivery of human fibroblast cells by piezoelectric drop-on-demand inkjet printing *Biomaterials* **29** 193–203
[27] Arai K, Iwanaga S, Toda H, Genci C, Nishiyama Y and Nakamura M 2011 Three-dimensional inkjet biofabrication based on designed images *Biofabrication* **3** 34113
[28] Phillippi J A, Miller E, Weiss L, Huard J, Waggoner A and Campbell P 2008 Microenvironments engineered by inkjet bioprinting spatially direct adult stem cells toward muscle- and bone-like subpopulations *Stem Cells* **26** 127–34
[29] Xu T, Jin J, Gregory C, Hickman J J and Boland T 2005 Inkjet printing of viable mammalian cells *Biomaterials* **26** 93–9
[30] Cui X, Dean D, Ruggeri Z M and Boland T 2010 Cell damage evaluation of thermal inkjet printed Chinese hamster ovary cells *Biotechnol. Bioeng.* **106** 963–9
[31] Cui X and Boland T 2009 Human microvasculature fabrication using thermal inkjet printing technology *Biomaterials* **30** 6221–7
[32] Gao G, Yonezawa T, Hubbell K, Dai G and Cui X 2015 Inkjet-bioprinted acrylated peptides and PEG hydrogel with human mesenchymal stem cells promote robust bone and cartilage formation with minimal printhead clogging *Biotechnol. J.* **10** 1568–77
[33] Xu C, Zhang M, Huang Y, Ogale A, Fu J and Markwald R R 2014 Study of droplet formation process during drop-on-demand Inkjetting of living cell-laden bioink *Langmuir* **30** 9130–8
[34] Xu T, Zhao W, Zhu J-M, Albanna M Z, Yoo J J and Atala A 2013 Complex heterogeneous tissue constructs containing multiple cell types prepared by inkjet printing technology *Biomaterials* **34** 130–9
[35] Cui X, Breitenkamp K, Finn M G, Lotz M and D'Lima D D 2012 Direct human cartilage repair using three-dimensional bioprinting technology *Tissue Eng.* A **18** 1304–12
[36] Nair K, Gandhi M, Khalil S, Yan K C, Marcolongo M, Barbee K and Sun W 2009 Characterization of cell viability during bioprinting processes *Biotechnol. J.* **4** 1168–77
[37] Calvert P 2001 Inkjet printing for materials and devices *Chem. Mater.* **13** 3299–305
[38] Kim J D, Choi J S, Kim B S, Chan Choi Y and Cho Y W 2010 Piezoelectric inkjet printing of polymers: stem cell patterning on polymer substrates *Polymer* **51** 2147–54
[39] Campbell P G, Miller E D, Fisher G W, Walker L M and Weiss L E 2005 Engineered spatial patterns of FGF-2 immobilized on fibrin direct cell organization *Biomaterials* **26** 6762–70
[40] Murphy S V and Atala A 2014 3D bioprinting of tissues and organs *Nat. Biotechnol.* **32** 773–85
[41] Guillotin B *et al* 2010 Laser assisted bioprinting of engineered tissue with high cell density and microscale organization *Biomaterials* **31** 7250–6
[42] Unger C, Gruene M, Koch L, Koch J and Chichkov B N 2011 Time-resolved imaging of hydrogel printing via laser-induced forward transfer *Appl. Phys.* A **103** 271–7
[43] Catros S, Guillotin B, Bačáková M, Fricain J-C and Guillemot F 2011 Effect of laser energy, substrate film thickness and bioink viscosity on viability of endothelial cells printed by laser-assisted bioprinting *Appl. Surf. Sci.* **257** 5142–7
[44] Guillemot F, Souquet A, Catros S and Guillotin B 2010 Laser-assisted cell printing: principle, physical parameters versus cell fate and perspectives in tissue engineering *Nanomedicine* **5** 507–15
[45] Duocastella M, Colina M, Fernández-Pradas J M, Serra P and Morenza J L 2007 Study of the laser-induced forward transfer of liquids for laser bioprinting *Appl. Surf. Sci.* **253** 7855–9
[46] Guillemot F *et al* 2010 High-throughput laser printing of cells and biomaterials for tissue engineering *Acta Biomater.* **6** 2494–500
[47] Barron J A, Wu P, Ladouceur H D and Ringeisen B R 2004 Biological laser printing: a novel technique for creating heterogeneous 3-dimensional cell patterns *Biomed. Microdevices* **6** 139–47
[48] Demirci U and Montesano G 2007 Single cell epitaxy by acoustic picolitre droplets *Lab. Chip* **7** 1139
[49] Chung J H Y, Naficy S, Yue Z, Kapsa R, Quigley A, Moulton S E and Wallace G G 2013 Bio-ink properties and printability for extrusion printing living cells *Biomater. Sci.* **1** 763

[50] Shor L, Güçeri S, Chang R, Gordon J, Kang Q, Hartsock L, An Y and Sun W 2009 Precision extruding deposition (PED) fabrication of polycaprolactone (PCL) scaffolds for bone tissue engineering *Biofabrication* **1** 15003
[51] Fedorovich N E, De Wijn J R, Verbout A J, Alblas J and Dhert W J A 2008 Three-dimensional fiber deposition of cell-laden, viable, patterned constructs for bone tissue printing *Tissue Eng.* A **14** 127–33
[52] Fedorovich N E, Schuurman W, Wijnberg H M, Prins H-J, van Weeren P R, Malda J, Alblas J and Dhert W J A 2012 Biofabrication of osteochondral tissue equivalents by printing topologically defined, cell-laden hydrogel scaffolds *Tissue Eng.* C **18** 33–44
[53] Smith C M, Stone A L, Parkhill R L, Stewart R L, Simpkins M W, Kachurin A M, Warren W L and Williams S K 2004 Three-dimensional bioassembly tool for generating viable tissue-engineered constructs *Tissue Eng.* **10** 1566–76
[54] Campos D F D, Blaeser A, Weber M, Jäkel J, Neuss S, Wilhelm J-D and Fischer H 2013 Three-dimensional printing of stem cell-laden hydrogels submerged in a hydrophobic high-density fluid *Biofabrication* **5** 15003
[55] Dababneh A B and Ozbolat I T 2014 Bioprinting technology: a current state-of-the-art review *J. Manuf. Sci. Eng.* **136** 61016
[56] Peltola S M, Melchels F P W, Grijpma D W and Kellomäki M 2008 A review of rapid prototyping techniques for tissue engineering purposes *Ann. Med.* **40** 268–80
[57] Chang R, Nam J and Sun W 2008 Effects of dispensing pressure and nozzle diameter on cell survival from solid freeform fabrication–based direct cell writing *Tissue Eng.* A **14** 41–8
[58] Wu W, DeConinck A J and Lewis J A 2011 Omnidirectional printing of 3d microvascular networks *Adv. Mater.* **23** H178–83
[59] Highley C B, Rodell C B and Burdick J A 2015 Direct 3d printing of shear-thinning hydrogels into self-healing hydrogels *Adv. Mater.* **27** 5075–9
[60] Ovsianikov A *et al* 2014 Laser photofabrication of cell-containing hydrogel constructs *Langmuir* **30** 3787–94
[61] Li J, Rossignol F and Macdonald J 2015 Inkjet printing for biosensor fabrication: combining chemistry and technology for advanced manufacturing *Lab Chip* **15** 2538–58
[62] Marga F, Jakab K, Khatiwala C, Shepherd B, Dorfman S, Bradley H, Colbert S and Forgacs G 2012 Toward engineering functional organ modules by additive manufacturing *Biofabrication* **4** 22001
[63] Billiet T, Gevaert E, De Schryver T, Cornelissen M and Dubruel P 2014 The 3D printing of gelatin methacrylamide cell-laden tissue-engineered constructs with high cell viability *Biomaterials* **35** 49–62
[64] Melchels F P W, Dhert W J A, Hutmacher D W and Malda J 2014 Development and characterisation of a new bioink for additive tissue manufacturing *J. Mater. Chem.* B **2** 2282
[65] Gao Q, He Y, Fu J, Liu A and Ma L 2015 Coaxial nozzle-assisted 3D bioprinting with built-in microchannels for nutrients delivery *Biomaterials* **61** 203–15
[66] Tan E Y S and Yeong W Y 2015 Concentric bioprinting of alginate-based tubular constructs using multi-nozzle extrusion-based technique *Int. J. Bioprint.* **1** 49–65
[67] Hopp B, Smausz T, Kresz N, Barna N, Bor Z, Kolozsvári L, Chrisey D B, Szabó A and Nógrádi A 2005 Survival and proliferative ability of various living cell types after laser-induced forward transfer *Tissue Eng.* **11** 1817–23
[68] Guillotin B and Guillemot F 2011 Cell patterning technologies for organotypic tissue fabrication *Trends Biotechnol.* **29** 183–90
[69] Fang Y, Frampton J P, Raghavan S, Sabahi-Kaviani R, Luker G, Deng C X and Takayama S 2012 Rapid generation of multiplexed cell cocultures using acoustic droplet ejection followed by aqueous two-phase exclusion patterning *Tissue Eng.* C **18** 647–57
[70] Mignon A, Graulus G-J, Snoeck D, Martins J, De Belie N, Dubruel P and Van Vlierberghe S 2015 pH-sensitive superabsorbent polymers: a potential candidate material for self-healing concrete *J. Mater. Sci.* **50** 970–9
[71] Van Vlierberghe S, Dubruel P and Schacht E 2011 Biopolymer-based hydrogels as scaffolds for tissue engineering applications: a review *Biomacromolecules* **12** 1387–408
[72] Ullah F, Othman M B H, Javed F, Ahmad Z and Akil H M 2015 Classification, processing and application of hydrogels: a review *Mater. Sci. Eng.* C **57** 414–33
[73] Vlierberghe S V, Schacht E and Dubruel P 2011 Reversible gelatin-based hydrogels: finetuning of material properties *Eur. Polym. J.* **47** 1039–47
[74] Fu Y and Kao W J 2011 *In situ* forming poly(ethylene glycol)-based hydrogels via thiol-maleimide Michael-type addition *J. Biomed. Mater. Res.* A **98A** 201–11
[75] Sivashanmugam A, Arun Kumar R, Vishnu Priya M, Nair S V and Jayakumar R 2015 An overview of injectable polymeric hydrogels for tissue engineering *Eur. Polym. J.* **72** 543–65
[76] Moreira Teixeira L S, Feijen J, van Blitterswijk C A, Dijkstra P J and Karperien M 2012 Enzyme-catalyzed crosslinkable hydrogels: emerging strategies for tissue engineering *Biomaterials* **33** 1281–90
[77] Ovsianikov A, Deiwick A, Van Vlierberghe S, Pflaum M, Wilhelmi M, Dubruel P and Chichkov B 2011 Laser fabrication of 3D gelatin scaffolds for the generation of bioartificial tissues *Materials* **4** 288–99
[78] Li C *et al* 2015 Rapid formation of a supramolecular polypeptide-dna hydrogel for *in situ* three-dimensional multilayer bioprinting *Angew. Chem., Int. Ed. Engl.* **54** 3957–61
[79] Graulus G-J, Mignon A, Van Vlierberghe S, Declercq H, Fehér K, Cornelissen M, Martins J C and Dubruel P 2015 Cross-linkable alginate-graft-gelatin copolymers for tissue engineering applications *Eur. Polym. J.* **72** 494–506
[80] Skardal A, Zhang J, McCoard L, Xu X, Oottamasathien S and Prestwich G D 2010 Photocrosslinkable hyaluronan-gelatin hydrogels for two-step bioprinting *Tissue Eng.* A **16** 2675–85
[81] Colosi C, Shin S R, Manoharan V, Massa S, Costantini M, Barbetta A, Dokmeci M R, Dentini M and Khademhosseini A 2016 Microfluidic bioprinting of heterogeneous 3D tissue constructs using low-viscosity bioink *Adv. Mater.* **28** 677–84
[82] Choi Y C, Choi J S, Kim B S, Kim J D, Yoon H I and Cho Y W 2012 Decellularized extracellular matrix derived from porcine adipose tissue as a xenogeneic biomaterial for tissue engineering *Tissue Eng.* C **18** 866–76
[83] Xu T, Molnar P, Gregory C, Das M, Boland T and Hickman J J 2009 Electrophysiological characterization of embryonic hippocampal neurons cultured in a 3D collagen hydrogel *Biomaterials* **30** 4377–83
[84] Van Den Bulcke A I, Bogdanov B, De Rooze N, Schacht E H, Cornelissen M and Berghmans H 2000 Structural and rheological properties of methacrylamide modified gelatin hydrogels *Biomacromolecules* **1** 31–8
[85] Collins M N and Birkinshaw C 2013 Hyaluronic acid based scaffolds for tissue engineering—a review *Carbohydr. Polym.* **92** 1262–79
[86] Oudshoorn M H M, Rissmann R, Bouwstra J A and Hennink W E 2007 Synthesis of methacrylated hyaluronic acid with tailored degree of substitution *Polymer* **48** 1915–20
[87] Masters K S, Shah D N, Leinwand L A and Anseth K S 2005 Crosslinked hyaluronan scaffolds as a biologically active carrier for valvular interstitial cells *Biomaterials* **26** 2517–25
[88] Bryant S J, Nicodemus G D and Villanueva I 2008 Designing 3D photopolymer hydrogels to regulate biomechanical cues and tissue growth for cartilage tissue engineering *Pharm. Res.* **25** 2379–86
[89] Aguado B A, Mulyasasmita W, Su J, Lampe K J and Heilshorn S C 2012 Improving viability of stem cells during syringe needle flow through the design of hydrogel cell carriers *Tissue Eng.* A **18** 806–15

[90] Schuurman W, Levett P A, Pot M W, van Weeren P R, Dhert W J A, Hutmacher D W, Melchels F P W, Klein T J and Malda J 2013 Gelatin-methacrylamide hydrogels as potential biomaterials for fabrication of tissue-engineered cartilage constructs: gelatin-methacrylamide hydrogels as potential biomaterials for fabrication … *Macromol. Biosci.* **13** 551–61
[91] Mihaila S M, Gaharwar A K, Reis R L, Marques A P, Gomes M E and Khademhosseini A 2013 Photocrosslinkable kappa-carrageenan hydrogels for tissue engineering applications *Adv. Healthc. Mater.* **2** 895–907
[92] Guvendiren M, Lu H D and Burdick J A 2011 Shear-thinning hydrogels for biomedical applications *Soft Matter* **8** 260–72
[93] Ovsianikov A, Mironov V, Stampfl J and Liska R 2012 Engineering 3D cell-culture matrices: multiphoton processing technologies for biological and tissue engineering applications *Expert Rev. Med. Devices* **9** 613–33
[94] Talbot E L, Berson A, Brown P S and Bain C D 2012 Evaporation of picoliter droplets on surfaces with a range of wettabilities and thermal conductivities *Phys. Rev.* E **85** 61604
[95] Levato R, Visser J, Planell J A, Engel E, Malda J and Mateos-Timoneda M A 2014 Biofabrication of tissue constructs by 3D bioprinting of cell-laden microcarriers *Biofabrication* **6** 35020
[96] Skardal A *et al* 2015 A hydrogel bioink toolkit for mimicking native tissue biochemical and mechanical properties in bioprinted tissue constructs *Acta Biomater.* **25** 24–34
[97] Van Hoorick J, Declercq H, De Muynck A, Houben A, Van Hoorebeke L, Cornelissen R, Van Erps J, Thienpont H, Dubruel P and Van Vlierberghe S 2015 Indirect additive manufacturing as an elegant tool for the production of self-supporting low density gelatin scaffolds *J. Mater. Sci., Mater. Med.* **26** 247
[98] Van Vlierberghe S, Dubruel P, Lippens E, Masschaele B, Van Hoorebeke L, Cornelissen M, Unger R, Kirkpatrick C J and Schacht E 2008 Toward modulating the architecture of hydrogel scaffolds: curtains versus channels *J. Mater. Sci., Mater. Med.* **19** 1459–66
[99] Hsieh F-Y, Lin H-H and Hsu S 2015 3D bioprinting of neural stem cell-laden thermoresponsive biodegradable polyurethane hydrogel and potential in central nervous system repair *Biomaterials* **71** 48–57
[100] Markstedt K, Mantas A, Tournier I, Martínez Ávila H, Hägg D and Gatenholm P 2015 3D bioprinting human chondrocytes with nanocellulose–alginate bioink for cartilage tissue engineering applications *Biomacromolecules* **16** 1489–96
[101] Das S, Pati F, Choi Y-J, Rijal G, Shim J-H, Kim S W, Ray A R, Cho D-W and Ghosh S 2015 Bioprintable, cell-laden silk fibroin–gelatin hydrogel supporting multilineage differentiation of stem cells for fabrication of three-dimensional tissue constructs *Acta Biomater.* **11** 233–46
[102] Yan C, Mackay M E, Czymmek K, Nagarkar R P, Schneider J P and Pochan D J 2012 Injectable solid peptide hydrogel as a cell carrier: effects of shear flow on hydrogels and cell payload *Langmuir* **28** 6076–87
[103] Lu H D, Charati M B, Kim I L and Burdick J A 2012 Injectable shear-thinning hydrogels engineered with a self-assembling Dock-and-Lock mechanism *Biomaterials* **33** 2145–53
[104] Okay O 2009 *General Properties of Hydrogels Hydrogel Sensors and Actuators* ed G Gerlach and K-F Arndt vol 6 (Berlin, Heidelberg: Springer) pp 1–14
[105] Bencherif S A, Srinivasan A, Horkay F, Hollinger J O, Matyjaszewski K and Washburn N R 2008 Influence of the degree of methacrylation on hyaluronic acid hydrogels properties *Biomaterials* **29** 1739–49
[106] Shim J-H, Kim J Y, Park M, Park J and Cho D-W 2011 Development of a hybrid scaffold with synthetic biomaterials and hydrogel using solid freeform fabrication technology *Biofabrication* **3** 34102
[107] Gladman A S, Matsumoto E A, Nuzzo R G, Mahadevan L and Lewis J A 2016 Biomimetic 4D printing *Nat. Mater.* **12** 413–8
[108] Klein T J, Rizzi S C, Reichert J C, Georgi N, Malda J, Schuurman W, Crawford R W and Hutmacher D W 2009 Strategies for zonal cartilage repair using hydrogels *Macromol. Biosci.* **9** 1049–58
[109] Skardal A, Zhang J and Prestwich G D 2010 Bioprinting vessel-like constructs using hyaluronan hydrogels crosslinked with tetrahedral polyethylene glycol tetracrylates *Biomaterials* **31** 6173–81
[110] Buckley C T, Thorpe S D, O'Brien F J, Robinson A J and Kelly D J 2009 The effect of concentration, thermal history and cell seeding density on the initial mechanical properties of agarose hydrogels *J. Mech. Behav. Biomed. Mater.* **2** 512–21
[111] Guilak F, Jones W R, Ting-Beall H P and Lee G M 1999 The deformation behavior and mechanical properties of chondrocytes in articular cartilage *Osteoarthr. Cartil. OARS Osteoarthr. Res. Soc.* **7** 59–70
[112] Almeida H A and Bártolo P J 2013 Numerical simulations of bioextruded polymer scaffolds for tissue engineering applications: numerical simulations of bioextruded polymer scaffolds *Polym. Int.* **62** 1544–52
[113] Chantarapanich N, Puttawibul P, Sucharitpwatskul S, Jeamwatthanachai P, Inglam S and Sitthiseripratip K 2012 Scaffold library for tissue engineering: a geometric evaluation *Comput. Math. Methods Med.* **2012** 1–14
[114] Hollister S J 2005 Porous scaffold design for tissue engineering *Nat. Mater.* **4** 518–24
[115] Hutmacher D W, Sittinger M and Risbud M V 2004 Scaffold-based tissue engineering: rationale for computer-aided design and solid free-form fabrication systems *Trends Biotechnol.* **22** 354–62
[116] Bae H, Ahari A F, Shin H, Nichol J W, Hutson C B, Masaeli M, Kim S-H, Aubin H, Yamanlar S and Khademhosseini A 2011 Cell-laden microengineered pullulan methacrylate hydrogels promote cell proliferation and 3D cluster formation *Soft Matter* **7** 1903
[117] Cha C, Shin S R, Gao X, Annabi N, Dokmeci M R, Tang X S and Khademhosseini A 2014 Controlling mechanical properties of cell-laden hydrogels by covalent incorporation of graphene oxide *Small* **10** 514–23
[118] Lee B-H, Li B and Guelcher S A 2012 Gel microstructure regulates proliferation and differentiation of MC3T3-E1 cells encapsulated in alginate beads *Acta Biomater.* **8** 1693–702
[119] Mauck R L, Wang C-B, Oswald E S, Ateshian G A and Hung C T 2003 The role of cell seeding density and nutrient supply for articular cartilage tissue engineering with deformational loading *Osteoarthr. Cartil.* **11** 879–90
[120] Chang S C, Rowley J A, Tobias G, Genes N G, Roy A K, Mooney D J, Vacanti C A and Bonassar L J 2001 Injection molding of chondrocyte/alginate constructs in the shape of facial implants *J. Biomed. Mater. Res.* **55** 503–11
[121] Guilak F and Mow V C 2000 The mechanical environment of the chondrocyte: a biphasic finite element model of cell-matrix interactions in articular cartilage *J. Biomech.* **33** 1663–73
[122] Chang Yan K, Nair K and Sun W 2010 Three dimensional multi-scale modelling and analysis of cell damage in cell-encapsulated alginate constructs *J. Biomech.* **43** 1031–8
[123] Markovic M, Van Hoorick J, Hölzl K, Tromayer M, Gruber P, Nürnberger S, Dubruel P, Van Vlierberghe S, Liska R and Ovsianikov A 2015 Hybrid tissue engineering scaffolds by combination of three-dimensional printing and cell photoencapsulation *J. Nanotechnol. Eng. Med.* **6** 21004
[124] Takai E, Costa K D, Shaheen A, Hung C T and Guo X E 2005 Osteoblast elastic modulus measured by atomic force microscopy is substrate dependent *Ann. Biomed. Eng.* **33** 963–71
[125] Steinmetz N J, Aisenbrey E A, Westbrook K K, Qi H J and Bryant S J 2015 Mechanical loading regulates human MSC differentiation in a multi-layer hydrogel for osteochondral tissue engineering *Acta Biomater.* **21** 142–53
[126] Carlier A, Geris L, Lammens J and Van Oosterwyck H 2015 Bringing computational models of bone regeneration to the clinic: bringing computational models of bone

regeneration to the clinic *Wiley Interdiscip. Rev. Syst. Biol. Med.* **7** 183–94

[127] Eshraghi S and Das S 2012 Micromechanical finite-element modeling and experimental characterization of the compressive mechanical properties of polycaprolactone–hydroxyapatite composite scaffolds prepared by selective laser sintering for bone tissue engineering *Acta Biomater.* **8** 3138–43

[128] Díaz-Zuccarini V and Lawford P V 2010 An in silico future for the engineering of functional tissues and organs *Organogenesis* **6** 245–51